



Identification of the state-space dynamics of oil flames through computer vision and modal techniques

R.P. Silva ^{a,1}, A.T. Fleury ^{b,2}, F.P.R. Martins ^{a,3}, W.J.A. Ponge-Ferreira ^{a,3}, F.C. Trigo ^{a,*}

^a Escola Politécnica da Universidade de São Paulo, Departamento de Engenharia Mecânica, Av. Prof. Mello Moraes 2231, São Paulo, SP 05508-930, Brazil

^b Centro Universitário da FEI, Av. Humberto de Alencar Castelo Branco, 3972, São Bernardo do Campo, SP 09850-901, Brazil



ARTICLE INFO

Article history:

Available online 4 November 2014

Keywords:

Flame instabilization characterizing
Operational Modal Analysis
Discriminant characteristic vectors
Artificial intelligence image processing

ABSTRACT

In industrial oil furnaces, unstable flames can lead to potentially dangerous conditions. For this reason, elaborate control systems are used to monitor the various parameters of the process that could become the source of such problems. A current trend in research is the one that seeks to apply artificial intelligence techniques to efficiently identify *a priori* anomalous behavior of the flames, so as to help improving the time response of the automatic control. In system dynamics theory, it is common sense that an accurate modeling of the process under study directly affects the performance of the controlling apparatus. Unfortunately, due to the complexity of the process, physical models of flame propagation are still not as much faithful as they should to be used for control purposes. On the other hand, could the complex dynamics of flame propagation be described in terms of an identified assumed model, one would come up with a tool for the improvement of the control strategy. In this work, a new approach based on Operational Modal Analysis (OMA) tools is used to identify four degree-of-freedom second order state-space models of oil flame dynamics in a prototype furnace. Grabbed images of a CCD camera, after being processed through a computer vision method, provide sets of characteristic vectors which, then, serve as input data to an identification OMA algorithm based on the Ibrahim Time Domain Method. Models of unstable and stable flames are built and validated through spectral analysis of the reconstructed time-domain characteristic vectors. The truthfulness of the validation scheme was then confirmed by a quantitative modal assurance criterion modified to suit the current application. On the grounds of the results obtained, it is possible to assert that the proposed approach for the description of flame dynamics can likely predict the occurrence of unstable conditions, thus becoming another tool that might be used in an automated control system.

© 2014 Elsevier Ltd. All rights reserved.

1. Introduction

The monitoring of oil-flame conditions in industrial petrochemical plants is of capital importance in terms of economy, environment-friendly operation, and safety. Currently, a wide array of sensors performs the task of measuring and informing the plant staff who, ultimately, judges the necessity of intervening to alter control parameters. This process has two drawbacks: firstly, sensors like thermocouples, flow meters, opacity meters, pressure

sensor or even air-fuel ratio gauges are normally expensive and require frequent maintenance interventions; secondly, the judging ability of distinct operators is not the same, which might lead to below-standard functioning condition, including potentially dangerous ones. The first drawback pointed above should be tackled by replacing the specialized sensors by a frame-grabber and a set of low-cost CCD video cameras properly inserted in the furnace; those cameras can produce a continuous flow of flame images exhibiting luminance patterns that are well correlated to the physical combustion variables. The second drawback can be handled with computer vision routines able to identify normal or abnormal combustion states through the analysis of the sequence of flame images grabbed by the cameras. However, such an aim cannot be successfully achieved unless the decision-making be supported by reliable inferences on the image processed data. That is why the computer vision based systems for combustion processes monitoring usually apply a heterogeneous set of statistical and artificial

* Corresponding author. Tel.: +55 11 30915334; fax: +55 11 30915687.

E-mail addresses: rodrigopradosilva@gmail.com (R.P. Silva), agfleury@fei.edu.br (A.T. Fleury), flavius.martins@usp.br (F.P.R. Martins), ponce@usp.br (W.J.A. Ponge-Ferreira), trigo.flavio@usp.br (F.C. Trigo).

¹ Tel.: +55 11 30915334; fax: +55 11 30915687.

² Tel./fax: +55 11 46165429.

³ Tel.: +55 11 30919648; fax: +55 11 30915687.

intelligence techniques, especially multivariate statistics, artificial neural networks and fuzzy logics.

Expert systems with these attributes are getting more and more importance for the oil and gas industries in the last years because of the potential impact to clean combustion. Some of the most recent contributions to this new area are presented in the sequence.

Taking into account that proper identification of coal chemical composition is essential to apply an optimization policy for a coal based combustion process, Zhou et al. (2014) implemented a computer vision method that used flame images analysis to perform the coal classification. In order to achieve such an aim, characteristic vectors of grabbed and averaged RGB flame images related to specific coal combustion processes were constructed using spatial and temporal features of the intensity image signals as well as their R and G/B channels. Then, a series of experiments concerning combustion processes based on 4 different chemical compositions of coal gave rise to a total of 384 feature vectors, from which 2/3 were used in the training of a support vector machine classification algorithm. Further validation tests showed that the accuracy of the implemented method surpassed 80% in all tested cases.

Gómez, Hernandez, Coello, Ronquillo, and Trejo (2013) proposed an artificial intelligence based method to identify 4 states of combustion processes – 'background radiation', 'stable flame', 'flame with air excess' and 'flame with fuel excess'. Using an optical sensor scanning system to record time series for the average levels of luminance of the furnace concerning the four states mentioned above, the authors construct feature vectors encompassing geometrical and statistical parameters extracted from these signals and their respective power spectra. Those feature vectors were further used to implement a supervised learning process based on a 2-layer MLP neural network whose internal weights were adjusted by a genetic algorithm aiming at improving its generalization capability.

Applying a cascade of statistical and image processing methods, Lin and Jorgensen (2011) synthesized a software based sensor to estimate the NOx emission rate of cement kiln processes. The methodology adopted by those authors consisted in constructing a partial least squares regression model that correlates the characteristic vectors extracted from the two most relevant eigen-images of each RGB flame image with the respective outputs of a set of sensors measuring chemical and physical variables of the process.

Sun, Lu, Zhou, and Yan (2011) carried out laboratorial experiments aiming at identifying parameters that could be related to instability in gaseous flames. After grabbing average images of flames due to combustion processes with different fuel/air ratios, encompassing fuel-lean and fuel-rich conditions, the authors examined the power spectra densities (PSDs) of both the visible and the infrared images. The PSD average frequencies versus fuel/air ratio graphs, from under stoichiometric (unstable flames) to upper stoichiometric (stable flames) conditions, exhibit an easily identifiable maximum (the stoichiometric condition) that can be used as a threshold to identify unstable flames.

In the article of Chen, Chang, and Cheng (2013) a new method of controlling the oxygen fuel rate as well its variability is proposed in order to improve the performance of industrial combustion processes. This method uses PCA compacted sequential sets of RGB flame images to generate measurements representing their main visual characteristics. According to the authors, almost 99% of the variance of the images is encompassed by the two most significant eigen-images of the set, two variables – the weights of those eigen-images – are used as observable variables on a two-loop control system developed to maintain a combustion furnace operating at an optimal and stable condition.

A key feature that must be monitored in order to maintain optimal burning conditions of oil flames is the vapor to fuel rate (VFR),

which directly affects fuel nebulization and flame quality. Fleury, Trigo, and Martins (2013) proposed a method based on computer vision and Kalman filtering to monitor nebulization quality of oil flames in a prototype refinery furnace. In short, the authors show that CCD-grabbed images of the flames at a priori known nebulization quality can be used to devise characteristic vectors that generate a set of fuzzy classification rules. Then, the components of a characteristic vector obtained from grabbed images of unknown a priori nebulization quality are assumed to be state-variables of a random-walk state-space model which, through a Kalman filter, effectively estimates the state and the nebulization quality when there is a statistically-proven convergence to a state that matches one of the classification rules. The researchers also state that the method could be improved once, instead of a random-walk model for the evolution of the state, a more accurate description of the system dynamics was employed. The difficulty that arises concerns the fact that phenomenological models available in the literature are poorly capable of encompassing both micro and macro scales occurring in flame propagation. As a consequence, a description based on either one would not cover the wide range of phenomena in between limiting conditions, thus resulting in a poor model under the estimation perspective.

Wang and Ren (2014) used a combined gray-level co-occurrence matrix of flame images and generalized learning vector neural network to estimate rotary kiln combustion characteristics. Texture features of images of flames with ideal working conditions comprised a database employed to train the neural network which, further on, was able to identify complete or incomplete combustion on test images.

In order to distinguish the combustion and ignition characteristics of natural gas components, and the effects of mixture blending, Kamada, Nakamura, Tesuka, Hasegawa, and Maruta (2014) studied the weak flame propagation in a reactor with controlled temperature conditions. Flame dynamics were numerically simulated and experimentally validated against the research octane numbers of each component fuel. Images of the weak flame propagation were grabbed at the experimental setup and, along with wall temperature measurements, provided the necessary data to validate the procedure. It must be pointed out that this important contribution does not employ any kind of automated expert system in the classification process; thus, the reference is justified under the perspective of using images to obtain characteristics of complex systems. Image and expert systems are also present in the work by Tomasoni, Saracoglu, and Paniagua (2014), who devised a flow pattern recognition algorithm in high-speed imaging to detect vortex-shedding and shock waves in ultrasonic air flow.

Another important issue for the adequate operation of refinery furnaces is the early detection of flame instability. This phenomenon may cause the extinction of the flame, resulting in an undesirable dangerous condition. Models for combustion instability in the literature (Bouziani, Landau, Bitmead, & Voda-Besancón, 2005) based on coupled van der Pol equations state that unstable conditions can be detected under certain controlled situations; however, perturbations may induce false instability diagnosis near theoretically stable operation setups. Therefore, a description of the dynamics of the system based purely on data from observations of flames under actual operating conditions could possibly enhance the predictability of AI algorithms in general. In dynamics, a technique that suits this purpose is Operational Modal Analysis (OMA) in the time domain.

Overall, OMA seeks to identify parameters of an assumed model of the system dynamics using information from measurements of the system response to known particular inputs, namely, either step or impulse excitations, in real operating environment. The so called Ibrahim Time-Domain Method (ITDM), one of the tools available to perform the task, is widely employed in the identification of frequencies and modes of vibration in structures like stayed

bridges (Liu et al., 2012; Wu, Chen, & Liao, 2012), offshore platforms (Wang, Zhang, & Feng, 2010), and components of rotating mechanisms (Grange, Clair, Baillet, & Fogli, 2009), just to cite some of the most recent publications.

An unconventional application of the ITDM was presented by Moura, Aya, Fleury, Amato, and Lima (2010). Those researchers employed the technique to identify the discrete state transition matrix in electrical impedance tomography, one of the instances for which analytical models do not suffice to describe the evolution of the state, the resistivity distribution in a domain of interest, with the required accuracy. This suggests the power of the ITDM, in the sense of surpassing its original scope, once the modal decomposition approach enables avoiding complex (and, sometimes, quite inaccurate) modeling, even of highly non-linear systems.

Considering the previous discussion and the importance of combustion condition monitoring, this paper proposes an extension of the work by the same authors (Fleury et al., 2013) which addresses the problem of detecting evidence of the beginning of flame unstable behavior (in order to avoid such condition) in the time domain. The ITDM framework is tailored to infer the state transition matrix from a four-degree of freedom second order model of this phenomenon in a prototype furnace. Grabbed images from a CCD camera are mapped into a state vector through computer vision methods. This new approach, once implemented in conjunction with AI algorithms, intends to improve the accuracy of the decision process.

In the next sections, data collection and processing, as well as a brief description of the ITDM, with emphasis on the current approach are presented.

2. Methods

The experimental set up that simulates a small-scale refinery furnace and the image data acquisition equipment are the same as mentioned by Fleury et al. (2013), reason why, in this paper, only a concise description is provided. In Fig. 1, the lower part of the vertical 4-meter high prototype furnace is depicted, with the burner schematics shown in detail. The CCD camera for image grabbing is placed in a shielded and cooled compartment in the central cross-section of the furnace cylindrical wall. Burner inlets of primary and dry air, steam and oil enable the control of combustion parameters.

In order to correlate the visual appearance of the flames with the stability of the combustion process, three series of operational tests were carried out. Typical stability states, ranked according to a specialist, were obtained through proper regulation of the primary/secondary air rate (PSAR) at the burner nozzle, as depicted in the detail of Fig. 1. Those series, encompassing an amount of 280 images, will be nominated hereafter as 'stable flames (PSAR = 1.0)',

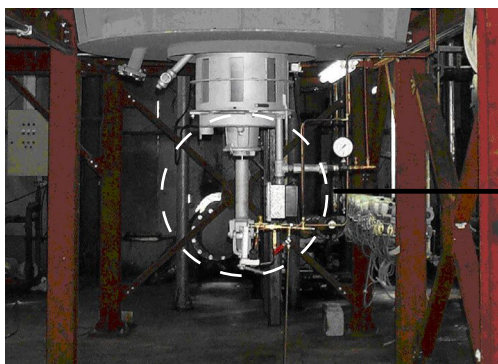


Fig. 1. Burner schematics (modified from Fleury et al. (2013)).

'unsteady flames (PSAR = 1.86)' and 'unstable flames (PSAR = 4.0)'. As illustrated by Fig. 2(a)–(c), the visual appearance of those image flames are clearly distinct, since the spatial distribution and arrangement of their pixel gray levels give rise to different types of texture.

The previous assertion was taken into account to construct a discriminant characteristic vector \vec{v}_i based on 13 properties directly related to the texture and spatial distribution of the pixel gray levels of the flame image I_i . The components of \vec{v}_i correspond to the following image properties:

- $v_i[1]$ is the average pixel gray level;
- $v_i[2]$ is the image entropy: $v_i[2] = -\sum_{j=1}^N p_j \log_2(p_j)$, where p_j is the frequency occurrence of gray level j ;
- $v_i[3]$ is the average local maximum pixel gray level difference observed through a complete image scanning by a 3×3 window;
- $v_i[4]$ is the average local maximum mean standard deviation observed through a complete image scanning by a 3×3 window;
- $v_i[5]$ to $v_i[13]$ are texture characteristics based on the co-occurrence matrix (Gonzalez & Woods, 1992) of the image I_i , relative to two horizontally neighbor pixels whose gray levels are separated by either 1, 3 or 5 units. This way, $v_i[5]$, $v_i[6]$, and $v_i[7]$ are the correlation indexes of the number of occurrences of sequences of two pixels i and j whose gray levels are separated by 1, 3 and 5 units, respectively. Those indexes are calculated according to

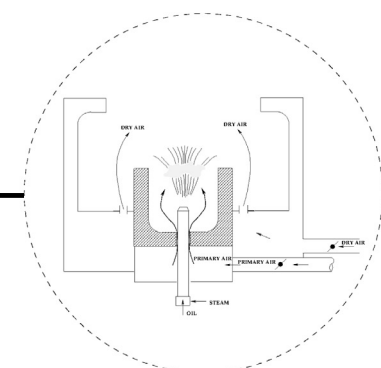
$$\sum_{i,j} \frac{(i - \mu_i)(j - \mu_j)p(i,j)}{\sigma_i \sigma_j} \quad (1)$$

where $p(i,j)$ is the frequency occurrence of two horizontally pixels exhibiting gray levels i and j , μ_i and μ_j are the average number of occurrences of gray level pixels i and j , and σ_i, σ_j are their corresponding mean standard deviation. Similarly, $v_i[8], v_i[9]$, and $v_i[10]$ are the contrast values of the number of occurrences of sequences of two pixels i and j whose gray levels are separated by 1, 3 and 5 units, respectively. Those indexes are calculated according to

$$\sum_{i,j} |i - j|^2 p(i,j) \quad (2)$$

Finally, $v_i[11], v_i[12]$, and $v_i[13]$ are the homogeneity values of the number of occurrences of sequences of two pixels i and j whose gray levels are separated by 1, 3 and 5 units, respectively. Those measures are calculated according to

$$\sum_{i,j} \frac{p(i,j)}{1 + |i - j|} \quad (3)$$



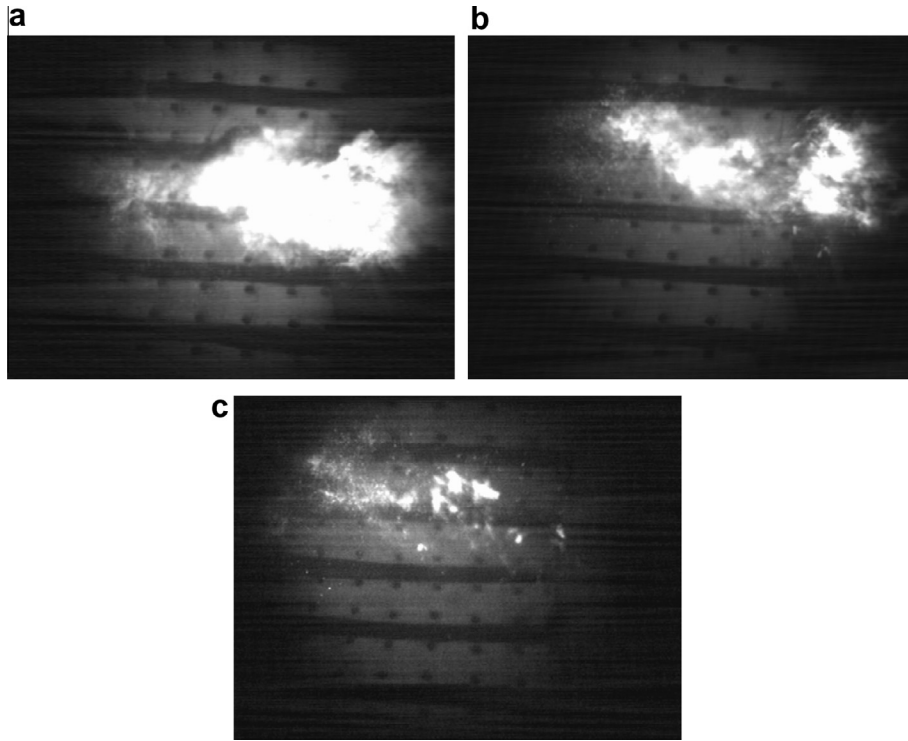


Fig. 2. Flame images. (a) PSAR = 1.0; (b) PSAR = 1.86; (c) PSAR = 4.0.

3. Ibrahim Time-domain Method theoretical background

The ITDM was conceived in the 1970s and has, since then, been developed and successfully applied. The methodology here presented is a concise version of a work by [Pappa and Ibrahim \(1981\)](#), which reviews a series of previous research since [Ibrahim and Mikulcik \(1973\)](#).

Essentially, as originally devised, the method infers modal properties of a n -degree of freedom 2nd order assumed model from the free-response of a system to either impulsive or other excitation function ([Ewins, 2000](#)). By hypothesis, the dynamics of the system is represented by the equation

$$My + C\dot{y} + Ky = f \quad (4)$$

in which M is the mass matrix, C is the damping matrix and K is the stiffness matrix, y, \dot{y}, \ddot{y} respectively represent displacement, velocity and acceleration vector, while f stands for the exogenous forcing vector. Once this model is mapped into a state-space framework and the resulting $2n$ first order differential equations are written in matrix form, a so called $2n \times 2n$ system matrix conveys all information concerning inertia, stiffness and damping characteristics of the system under analysis.

As it is known from dynamic system theory, the *eigenvalues* of the system matrix are used to compute natural frequencies and damping factors, whereas its *eigenvectors* provide mode shapes, for each degree-of-freedom of the assumed model. Thus, provided that the system undergoes free vibration, Ibrahim's method estimates the above-mentioned matrix. Thus, naming x the state vector and A the system matrix, for a certain instant t_i , a set of displacements, velocities and acceleration measurements of the free-response of the system yield n linear equations to solve for $2n^2$ unknowns according to Eq. (5),

$$\dot{x}_j = Ax_j \quad (5)$$

When measurements for $2n$ instants t_1, t_2, \dots, t_{2n} , are made, then one comes up with $2n^2$ equations, as follows:

$$[\dot{x}_1 \dot{x}_2 \dots \dot{x}_{2n}] = A[x_1 x_2 \dots x_{2n}] \quad (6)$$

$$\dot{X} = AX \rightarrow A = XX^{-1} \quad (7)$$

Hence, considering that all the components of X and dX/dt are available, matrix A is unambiguously obtained, as it can be realized from Eq. (12). It must be emphasized that the solution of this set of equations is accurate, since X and dX/dt matrices thus built are square. However, this approach demands the knowledge of displacements, velocities and accelerations at every instant, which requires integration and/or derivation of measured signals, or a complex sensing apparatus to read the three quantities. This disadvantage was overcome by [Pappa and Ibrahim \(1981\)](#), who improved the method to use either of the quantities for the estimation of the system matrix. To this end, regarding that the characteristic equation for the free-response of the system in Eq. (4) is

$$\lambda^2 M + \lambda C + K = 0 \quad (8)$$

the solution of Eq. (7), at any measuring spot j , may be written as the sum of the contribution of each individual mode at that spot; for a given instant t_j ,

$$x_j(t_i) = \sum_{k=1}^{2n} \psi_{jk} e^{\lambda_k t_i} \quad (9)$$

in which ψ_{jk} represents the free-response of the mode associated to the k th eigenvector at the j th spot, and λ_k the corresponding eigenvalue, solution of the characteristic equation, in general, both complex numbers. When $2n$ points are measured at several time instants, after some algebraic manipulation, [Pappa and Ibrahim \(1981\)](#) prove that the sought system matrix A is part of an eigenvalue problem. It follows that the eigenvalues of matrix A , complex numbers of the form $\lambda_k = \beta_k + i\gamma_k$, and the roots of the characteristic equation, the eigenvalues of the spatial model of Eq. (1) ([Ewins, 2000](#)) $s_k = \sigma_k + i\omega_{d,k}$, are related by

$$\beta_k + i\gamma_k = e^{\{\sigma_k + i\omega_{d,k}\}\Delta t_1} \quad (10)$$

In the above equation, Δt_1 represents an arbitrary time-shift and, in view of Eq. (9), the scalars β_k and γ_k can be used to obtain the damped natural frequency, natural frequency and damping factor for each mode according to Eqs. (11)–(14) below which, once associated to the eigenvectors, completely characterize the system dynamics.

$$\omega_{d,k} = \tan^{-1} \left(\frac{\gamma_k}{\beta_k} \right) \quad (11)$$

$$\zeta_k = \frac{\sigma_k}{(\sigma_k^2 + \omega_{d,k}^2)^{1/2}} \quad (12)$$

$$\omega_{n,k} = \frac{\omega_{d,k}}{(1 - \zeta_k^2)^{1/2}} \quad (13)$$

$$\sigma_k = \frac{1}{2\Delta t_1} \ln (\beta_k^2 + \gamma_k^2) \quad (14)$$

An important issue that avoids straightly employing either the original or the modified ITDM is the demand of data from the free-response of the system under evaluation. This problem arises in several field situations, for instance, the identification of large structures like buildings and bridges, whose free-response is virtually impossible to obtain since, at least, random excitation coming from the environment (wind, ground vibration transmitted to the structure *via* mechanical constraints) is always present. In the case of the present scope, a free-response would imply extinguishing the flame, a potentially dangerous operational condition. This difficulty can be surmounted when the ITDM is employed in conjunction with the Random Decrement Technique (Cole, 1971), also known as RANDOMDEC, since demonstrated by Ibrahim and Mikulcik (1977).

The RANDOMDEC technique uses data from random excitation to estimate the free-response of the system. Cole (1971) asserts that, for a system vibrating under random stationary excitation, when the average of numerous samples of the displacement response are computed, the contribution of velocities and accelerations on the measured signal gradually vanish; consequently, the free-response is obtained. The *RANDOMDEC signature* of the system, as named by Cole, is computed using segments of the measured displacement signal delimited by the same boundary condition (a chosen amplitude, for instance). First, N equal time-length τ segments of the measured signal $y(t)$, starting at instants t_j ($j = 1, 2, \dots, N$) provided that $y(t_j) = \alpha$ (the boundary condition) are sampled. Subsequently, the signature is obtained according to Eq. (15),

$$\delta(\tau) = \frac{1}{N} \sum_{j=1}^N y(t_j + \tau) \quad (15)$$

the sought free-response of the system.

In this work, the RANDOMDEC signature is computed from averages of segments with initial value (boundary condition) ranging from 60% to 80% of the maximum amplitude. A four degree-of-freedom second order system model with viscous damping was admitted for the application of the ITDM. Owing to the availability of only one measuring station (the housing for the camera in the furnace wall), the procedure outlined by Pappa and Ibrahim (1981) was employed to fill the response matrix and the time-shifted response matrix, in the following way: lines at the upper half of the response matrix received data collected at lagging intervals of 1/24 and 1/8 s; data on the upper four lines, further delayed in 7/24 s, completed the lower four lines. The lagged response matrix, on the other hand, was obtained through a time-shift of 5/6 s of the elements of the response matrix. Finally, 12 time-instants were used by the ITDM.

At this point, one might argue that the furnace/flame kept in steady operation does not characterize a random excitation. In

reply, one may assert that, for the observation model employed, i.e., grabbed images from a CCD camera, a deterministic excitation would be identifiable only if one directly altered luminous intensity inside the furnace, instead of acting on PSAR at the burner. Since the former is not done in the experiment, the hypothesis of random excitation holds.

4. Results and discussion

Grabbed images from the unstable flame condition (PSAR = 4.0) were processed according to the description of Section 2, providing a set of vectors $v_i(t_k)$, $i = 1, \dots, 13$, $k = 1, \dots, 100$, corresponding to a temporal sequence from available data of short-period trials for each of the 13 image characteristics. This reduced number of results poses another difficulty to the utilization of the RANDOMDEC technique: according to Cole (1971), the procedure is as accurate as the number of averages in Eq. (12) increases. One manner to deal with this problem is by vectorizing v_i so as to obtain a longer sequence and improve algorithm performance, an artifice whose justification is based on the rationale that follows.

In the first place, the stationarity hypothesis was admitted as a requirement to the RANDOMDEC scheme, which implies that grabbed data (images) represents a stochastic process. The instantaneous components of each of the characteristic vectors v_i are obtained from the same data sample through strictly deterministic algorithms; furthermore, this sample contains information concerning the whole process at that instant. Therefore, it is fair to admit that the process is also wide-sense ergodic. As a consequence, the proposed vectorization will preserve the two first moments of the entire process.

Off-set cancelation and normalization of each sequence of parameters were performed before the vectorization process, whose outcome for the PSAR = 4.0 is featured in Fig. 3. The 'relative amplitude' instead of physical units at the ordinates label is thereof justified. The RANDOMDEC/ITDM was, then, employed to compute the modal parameters of the model, which can be seen in the second and third columns of Table 1.

In order to corroborate the above results, a spectral analysis of the temporal sequence of Fig. 3 was performed and provided the power spectrum depicted in Fig. 4, on which is possible to realize the spreading of the signal power throughout the whole range of identifiable frequencies, namely, from 0 to 12 Hz, including peaks

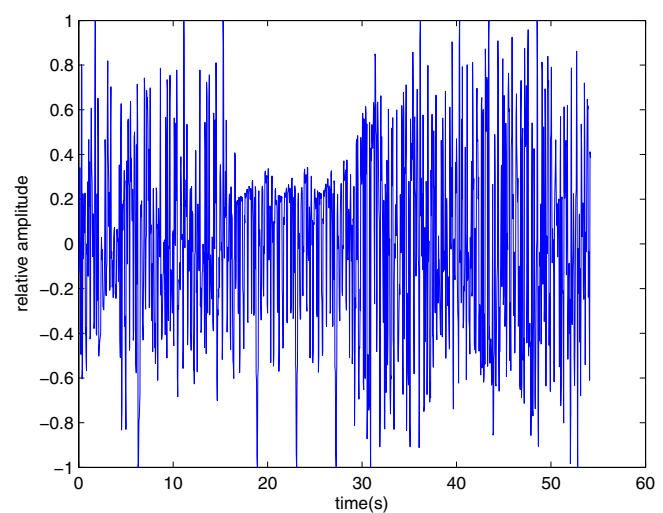


Fig. 3. Vectorized time-history of characteristic parameters for the 'unstable' flames (PSAR = 4.0).

Table 1

Damped natural frequencies/damping factors for each identified mode and discrepancy among frequencies computed from ITDM/RANDOMDEC and spectral analysis.

Natural mode	ITDM-Rd damped natural frequency f (Hz)/damping factor ζ	FFT damped natural frequency f (Hz)	$\frac{(f_{FFT} - f_{Rd/MI})}{f_{Rd/MI}} \times 100$
1	1.88/0.072	1.88	0.0
2	2.41/0.740	2.88	19.5
3	3.60/0.791	3.40	-5.5
4	5.03/0.005	5.07	-0.8

at the four frequencies obtained by the ITDM/RANDOMDEC technique. The occurrence of several spurious frequencies among those identified can be explained by leakage arising from the convolution with a rectangular window before the spectral analysis. Nevertheless, the four frequencies of interest do present higher relative amplitudes. For the sake of comparison, the third and fourth columns of **Table 1** show, respectively, natural frequencies computed by Fast Fourier Transform (FFT) and their relative discrepancy to the ones obtained with the proposed approach. Overall, the errors may be considered negligible except for the second natural mode.

The next step concerns the validation of the proposed approach; to this end, it suffices to verify whether data from stable (PSAR = 1.0) and partially stable (PSAR = 1.9) flame conditions, once processed according to ITDM/RANDOMDEC technique with parameters tuned for the unstable condition, can be distinguished from the latter. A further ratification is possible by reversing the process, i.e., using the ITDM/RANDOMDEC to identify stable flames and check the parameters thus found against partially stable and unstable flames. The results of both analyses are described below.

Spectra of signals reconstructed from the identified models, normalized by each relative amplitude, are depicted in **Fig. 4a** and b, whose reference spectra are respectively the curves for PSAR = 4 and PSAR = 1.0. According to common sense reasoning, one should expect closer resemblance between curves of PSARs 1.9 and 4.0 in **Fig. 4a** whereas, in **Fig. 4b**, curves of PSARs 1.9 and 1.0 would presumably look more alike. This qualitative analysis, however, does not provide solid ground for a definitive validation of the method since, in the first case, a clear match occurs once, at the 3.41 Hz frequency; on the other hand, in the second case, frequency matches occur close to abscissae 1.3 and 5.7 Hz.

A quantitative measure of the adherence between an estimated mode and a reference mode which is normally used in OMA is the

Modal Assurance Criterion – MAC (Ewins, 2000). The MAC essentially computes cumulative least-squares differences of all the combinations of pairs of data from distinct sets into a single scalar, despite that mode shapes and frequencies may be complex-valued. In the present case, the MAC has been modified to provide separate summations of the squared differences among frequencies and amplitudes of the reference and the other spectra in both cases under consideration.

Upon naming Nr : number of reference signals; Nt : number of test signals; Nrp : number of peaks of the reference signals; Ntp : number of peaks of the test signals; t : superscript related to test; r : superscript related to reference; F : computation index related to frequency; and A : computation index related to amplitude, the criterion can be mathematically stated according to:

$$(MAC_F)_{Nr} = \sum_{i=1}^{Nr} \sum_{j=1}^{Nrp} \sum_{k=1}^{Ntp} \left(F_{j,k}^t - F_{j,k}^r \right)_i^2, \quad Nr = 1, 2 \quad (16a)$$

$$(MAC_A)_{Nr} = \sum_{i=1}^{Nr} \sum_{j=1}^{Nrp} \sum_{k=1}^{Ntp} \left(A_{j,k}^t - A_{j,k}^r \right)_i^2, \quad Nr = 1, 2 \quad (16b)$$

$$MAC = 1 - \frac{MAC_F \times MAC_A}{\max(MAC_F, MAC_A)} \quad (16c)$$

Eqs. (16a) and (16b) represent a quantitative measure of the scattering of frequencies and relative amplitudes around respective their references, whereas Eq. (16c) expresses, in a single scalar, the combined effect of both dispersions. Thus, stable or partially stable flames, when tested using parameters computed from unstable flames, are expected to exhibit increasing values of MAC (partially stable > stable); conversely, unstable or partially stable flames should present decreasing values of MAC if probed against stable flames identified model. The results of the above validation are presented in **Table 2**, from which it is possible to confirm the truthfulness of those hypotheses.

The validation step ends the whole proposed process for detecting evidence of the beginning of flame instability. Recalling what was mentioned in the introductory section, it is now possible to collect, from Eq. (10), the proper components of the discrete-time state transition matrix A , thus characterizing the dynamics of the system in the time domain, as it was initially proposed. Moreover, time-history of characteristic vector can be reconstructed from the identified system model and, as a consequence, one is able to infer

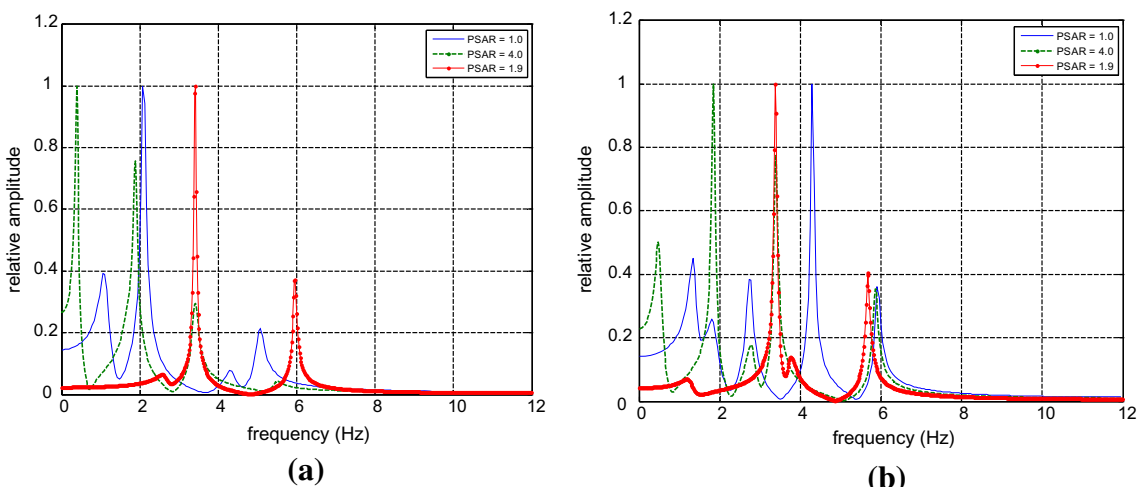
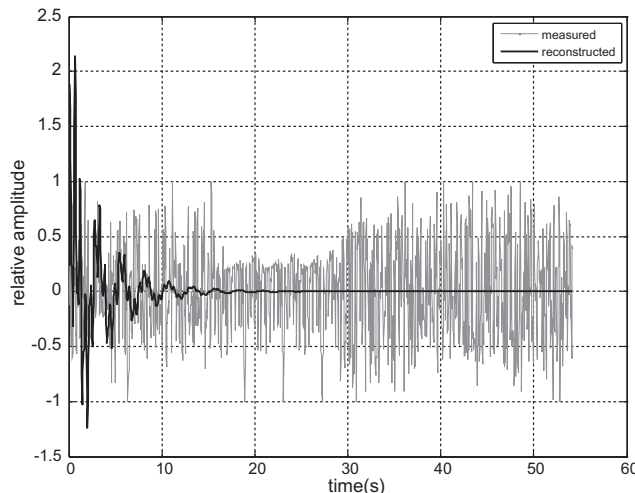


Fig. 4. Comparative relative power spectra for identified models of (a): unstable (PSAR = 4.0); and (b): stable (PSAR = 1.0) reference flames.

Table 2

MAC values for cross-validation of the qualitative analysis.

MAC	Test PSAR		
	1.0	1.9	4.0
Reference PSAR	4.0	0.0	0.67
	1.0	1.0	0.75
			0.0

**Fig. 5.** Comparative time-evolution of measured and reconstructed characteristic vectors for flames with PSAR = 4.0.

how long flames with those features would take to be extinguished. The time-evolution of both measured and reconstructed characteristic vectors is shown in Fig. 5, from which it can be asserted that unstable flames would last less than 20 s before total extinction.

It is important to point out that, in comparison to the previous work of Fleury et al. (2013), in which the white Gaussian noise represented the dynamics of flame propagation (in a state-space random walk model), the current research has been able to identify a second-order four degree-of-freedom model that describes the time evolution of the combustion process. Furthermore, data compression resulting from the application of modal identification, a feature that was not present in the previous work, tends to enhance the discrimination ability of the system, since redundancy is diminished.

5. Conclusions

The main contribution of the present work is the successful identification and validation of a grey-box model that is capable of describing the dynamics of oil-flames in a prototype furnace based on sequences of images grabbed by a CCD camera. The Operational Modal Analysis approach here adopted to quantitatively validate the procedure does not have, to the knowledge of the authors, any parallel in the literature. In relation to other works that attempt to infer evolution models from computer-vision processed images of turbulent phenomena (Chen et al. (2013), Tomasoni et al. (2014), for instance), the results here depicted overcome those in the sense that data compression through modal identification is likely to improve the discriminating ability of the flame classification system.

Concerning previous research by the same authors (Fleury et al., 2013), the superiority of the proposed scheme stems from the

development of a flame-image based dynamic model that can be used in the stochastic estimator instead of a random-walk model, thus improving the predictability of the said estimator.

As regards to the classification reliability provided by the method, results of the MAC criterion indicate that there is still room for improvement. The characteristic vector of the image could include temporal features such as the mean value and standard-deviation of the averaged light intensity, thus expanding the observability of the model. Furthermore, background removal (using, for example, time median filtering) would sever radiation of the instantaneous flames from that emitted by the refractory furnace wall. On the other hand, instead of inferring the parameters of a linear second-order grey-box model, a non-linear function could be probed in order to better describe the dynamics of the system in view of the observed data.

The above research suggestions and their incorporation in the methods already described comprise the core of current work by the authors of this article with the purpose of bringing about further improvements in decision-making algorithms to be used in automatic control systems for industrial applications.

References

Bouziani, F., Landau, I. D., Bitmead, R. R., Voda-Besançon, A. (2005). An analytically tractable model for combustion instability. In *Proceedings of the 44th IEEE conference on decision and control, and the European control conference 2005* (pp. 7398–7403). Seville, Spain.

Chen, J., Chang, Y. H., & Cheng, Y. C. (2013). Performance design of image-oxygen based cascade control loops for boiler combustion process. *Industrial and Engineering Chemistry Research*, 52(6), 2368–2378.

Cole, H. A. (1971). Failure Detection of a space shuttle wing flutter by random decrement. NASA, TMX-62.041.

Ewins, D. J. (2000). *Modal testing: Theory, practice and application* (2nd ed.). MTP: Hertsfordshire.

Fleury, A. T., Trigo, F. C., & Martins, F. P. R. (2013). A new approach based on computer vision and non-linear Kalman filtering to monitor the nebulization quality of oil flames. *Expert Systems with Applications*, 40(12), 4760–4769.

Gómez, J. C., Hernandez, F., Coello, C. A. C., Ronquillo, G., Trejo, A. (2013). Flame classification through the use of an artificial neural network trained with a genetic algorithm. In *Advances in soft computing and its applications. Lecture notes in computer science* (Vol. 8266, pp. 172–184).

Gonzalez, R. C., & Woods, R. E. (1992). *Digital image processing* (3rd ed.). New York: Addison-Wesley.

Grange, P., Clair, D., Baille, L., & Fogli, M. (2009). Brake squeal analysis by coupling spectral linearization and modal identification methods. *Mechanical Systems and Signal Processing*, 23(8), 2575–2589.

Ibrahim, S. R., & Mikulcik, E. C. (1973). A time domain modal vibration test technique. *The Shock and Vibration Bulletin*, 43(4), 21–37.

Ibrahim, S. R., & Mikulcik, E. C. (1977). A method for the direct identification of vibration parameters from the free response. *The Shock and Vibration Bulletin*, 47(4), 183–198.

Kamada, T., Nakamura, H., Tesuka, T., Hasegawa, S., & Maruta, K. (2014). Study on combustion and ignition characteristics of natural gas components in a micro flow reactor with a controlled temperature profile. *Combustion and Flame*, 161, 37–48.

Liu, T. Y., Chiang, W. L., Chen, C. W., Hsu, W. K., Lin, C. W., Chiou, D. J., et al. (2012). Structural system identification for vibration bridges using the Hilbert-Huang transform. *Journal of Vibration and Control*, 18(13), 1939–1956.

Lin, B., & Jorgensen, S. B. (2011). Soft sensor design by multivariate fusion of image features and process measurements. *Journal of Process Control*, 21, 347–353.

Moura, F. S., Aya, J. C. C., Fleury, A. T., Amato, M. B. P., & Lima, R. G. (2010). Dynamic imaging in electrical impedance tomography of the human chest with online transition matrix identification. *IEEE Transactions on Biomedical Engineering*, 57(2), 422–431.

Pappa, R. S., & Ibrahim, S. R. (1981). A parametric study of the Ibrahim time domain modal identification algorithm. *The Shock and Vibration Bulletin*, 51(3), 43–72.

Sun, D., Lu, G., Zhou, H., & Yan, Y. (2011). Flame stability monitoring and characterization through digital imaging and spectral analysis. *Measurement Science and Technology*, 22, 1–9.

Tomasoni, F., Saracoglu, B. H., & Panigagua, G. (2014). A decision-making algorithm for automatic flow pattern identification in high-speed imaging. *Expert Systems with Applications*, 41, 3935–3943.

Wu, W. H., Chen, C. C., & Liu, J. A. (2012). A multiple random decrement method for modal parameter identification of stay cables based on ambient vibration signals. *Advances in Structural Engineering*, 15(6), 969–982.

Wang, J. S., & Ren, X. D. (2014). GLCM based extraction of flame image texture features and KPCA-GLVQ recognition method for rotary kiln combustion working conditions. *International Journal of Automation and Computing*, 11(1), 72–77.

Wang, S. Q., Zhang, Y. T., Feng, Y. X. (2010). Comparative study of output-based modal identification methods using measured signals from an offshore platform. In *Proceedings of the ASME 29th international conference on ocean, offshore and arctic engineering* (Vol. 2, pp. 561–567).

Zhou, H., Tang, Q., Yang, L., Yan, Y., Lu, Gang, & Cen, K. (2014). Support vector machine based online coal identification through advanced flame monitoring. *Fuel*, 117, 944–951.